Comparative cyclotron resonance and luminescence study of photoexcited particles in mixed type-I–type-II GaAs/AlAs multiple quantum wells

M. Kozhevnikov, E. Cohen, and Arza Ron
Solid State Institute, Technion, Israel Institute of Technology, Haifa 32000, Israel

Hadas Shtrikman
Department of Condensed Matter Physics, The Weizmann Institute of Science, Rehovot 76100, Israel

L. N. Pfeiffer
Bell Laboratories, Murray Hill, New Jersey 07974

(Received 27 February 1997)

We report on the photoluminescence (PL) and photoinduced microwave absorption (PMA) of the elementary excitations in GaAs/AlAs undoped quantum wells (QW's) in the temperature range $2<T_L<30$ K. Mixed type-I–type-II QW's are used, since separate two-dimensional electron and hole gases are formed (in the wide and narrow QW's, respectively) by photoexcitation with densities in the range $10^9<n_e\leqslant 5\times10^{10}$ cm^{-2}. The PL spectra show transitions due to $(e1{:}\mathrm{hh}1)1S$ excitons (X) and $[(e1{:}\mathrm{hh}1)1S+e]$ negatively charged excitons (X^-). The PMA dependence on magnetic field that is applied perpendicularly to the QW planes shows cyclotron resonances (CR) due to electrons and X^- in the wide wells and heavy holes in the narrow wells. The CR traces are analyzed and yield the cyclotron effective mass, momentum relaxation rate, and relative density of the charged particles. The PL and PMA spectra are found to correlate well when observed at the same temperature and microwave power. The electron and X^- masses and relative intensities are analyzed in terms of weak in-plane particle localization. It is found that, at low temperatures, a large fraction of the electrons and X^- are localized by interface potential fluctuations. [S0163-1829(97)07528-0]

I. INTRODUCTION

The near-band-gap optical transitions of photoexcited quantum wells (QW's) that contain a two-dimensional electron gas (2DEG) depend on its density. Doped GaAs/Ga_xAl_{1-x}As QW's that have a high-density 2DEG ($n_e\geqslant10^{11}$ cm^{-2}) show a photoluminescence (PL) spectrum that is due to the recombination of unbound holes with free electrons.[1,2] In QW's that contain a 2DEG with $n_e<5\times10^{10}$ cm^{-2} and at low temperatures, the photoexcited e-h pairs form excitons whose binding energy and oscillator strength depend on n_e.[3–5] The absorption and PL spectra of the mixed phase, consisting of the 2DEG and the excitons, were studied both experimentally[3,5–7] and theoretically.[4,8,9] Recent studies[10–13] showed that, in addition to the $(e1{:}\mathrm{hh}1)1S$ exciton (X), this mixed phase sustains still another kind of particle: trion (X^-)—a bound $[(e1{:}\mathrm{hh}1)1S+e]$ exciton-electron complex. The X^- binding energy with respect to X is $\Delta E_{X^-}=E_{X^-}-E_X=1.15$ eV in GaAs wells of $\sim$200 Å width. Its energy levels, dependence on a magnetic-field applied perpendicularly to the QW plane, observed in PL spectra, verified its identification.[2,14] It was argued[11] that, in modulation-doped QW's, the X^- is localized by potential fluctuations that arise from the donor layer spatial fluctuations. This was based on correlating the vanishment of the dc conductivity with the appearance of the X^- PL line. Positively charged excitons (X^+) were observed[14,15] in the PL spectra of intentionally undoped and p-doped GaAs/$Al_{0.33}Ga_{0.67}$As multiple QW's (MQW's). The X^+ origin in undoped QW's was suggested to be in holes coming from background acceptors usually found in the barriers. It can thus be stated that charged excitons are intrinsic excitations of QW's that contain very low densities of either electrons or holes.

One of the methods used to study charged carrier transport properties (effective mass and mobility) in semiconducting QW's is the cyclotron resonance (CR). This is done either at microwave (mw) or at far-infrared (FIR) frequencies.[16,17] The mw CR study requires low magnetic fields ($B<1$ T) and has a number of distinctions from the FIR CR measurements (usually requiring $1<B<20$ T). Samples with a very high carrier mobility have to be used in order to satisfy the mw CR condition $\omega_c\tau\geqslant1$ at low magnetic fields ($\omega_c=eB/m^*$ is the cyclotron frequency and τ is the momentum relaxation time of the charged particle). Also, a large number of occupied Landau levels are involved in the mw CR, since the energy separation $\Delta E=\hbar\omega_c$ between adjacent Landau levels is usually smaller than both the carrier Fermi energy (E_F) and the thermal energy (k_BT_L). Indeed, assuming a low electron density of $n_e\sim2\times10^{10}$ cm^{-2}, $T_L=5$ K and $B\sim0.09$ T (the electron CR magnetic field at the mw frequency of 35.6 GHz that is used in this work), we obtain $\Delta E\sim0.15$ meV, $E_F\sim0.7$ meV, and $k_BT_L\sim0.4$ meV. This means that $n=4-6$ Landau levels are either fully or partially filled, and the CR band shape is determined by electron excitations from several Landau levels. It corresponds to a cyclotron radius of $r_{cr}=l_B\sqrt{2n+1}\sim1800$ Å, where $l_B=\sqrt{\hbar/eB}$ is the magnetic length. This experimental condition is termed ''classical'' CR ($\hbar\omega_c<k_BT_L$). On the other hand, when well-defined carrier tran-

sitions from the uppermost filled to the next empty Landau level occur, as is the case of FIR CR, the quantum limit is obtained ($\hbar\omega_c \gg k_B T_L$).

The main purpose of this paper is to report on a comparative study of the low-temperature photoinduced microwave absorption (PMA) and PL spectra in QW's containing a low-density photoexcited 2DEG. The PMA dependence on the magnetic field (applied perpendicularly to the QW plane) provides information on the charged particles: electrons, holes, and negatively charged excitons (X^-), through their CR. The PL spectra are due to the radiative recombination of the X, X^-, and holes interacting with the 2DEG. Therefore, our comparative study yields information on the state of all the particles present in the mixed phase consisting of the low-density photoexcited 2DEG, X, and X^-. This study was carried out mainly on mixed type-I–type-II GaAs/AlAs QW's (MTQW's) and, for reference, on conventional (type I) MQW's. The particular property of the MTQW's that makes them so useful in this research is the possibility to photoexcite spatially separated 2DEG and two-dimensional hole gas (2DHG). In addition, the gas density is easily controlled by the excitation intensity. Apart from a clear identification of the mixed phase constituents, our study provides information on the degree of electron and X^- localization in the QW plane.

The paper is laid out as follows: In Sec. II, the structure of the quantum wells, the experimental methods, and the experimental results are presented. In Sec. III, we analyze the correlation between the photoinduced microwave absorption and the photoluminescence spectra, the charged particle effective masses, and their momentum relaxation rates. Section IV is a summary of this paper.

II. QUANTUM-WELL STRUCTURES, EXPERIMENTAL PROCEDURE, AND RESULTS

Our study was conducted mainly on mixed type-I–type-II GaAs/AlAs quantum wells (MTQW's) grown on (001)-oriented GaAs substrates by molecular-beam epitaxy (MBE).[18] The MTQW consists of 30 periods of alternating wide (198 Å) and narrow (26 Å) GaAs wells that are separated by 102-Å-wide AlAs barriers. The reason for choosing this structure is that under photoexcitation into the narrow wells of the MTQW's [laser energy $E_L > E_g(e1\text{-hh1})_N \sim 1.9$ eV], electrons transfer rapidly (~ 30 psec) into the wide wells, forming a 2DEG there.[19,20] The holes tunnel slowly (~ 5 msec at a lattice temperature $T_L < 10$ K) and, thus, a separate 2DHG forms in the narrow wells. The 2DEG density is controlled by the laser intensity (I_L) in the range $10^9 \leqslant n_e \leqslant 5\times 10^{11}$ cm^{-2}.[13,21] We also studied a conventional (type I) GaAs/AlAs MQW that is used as a reference sample. It consists of 25 QW's of 202 Å width that are separated by 100-Å-wide AlAs barriers. This MQW was also grown on a (001)-oriented GaAs substrate by MBE.

The samples (with their substrate either thinned down to about 50 μm or completely removed by etching) were placed in a 35.6-GHz microwave cavity (at the antinode of the mw electric field). The cavity was mounted in an immersion-type Dewar and the sample temperature was varied in the range $T_L = 2-30$ K. A stabilized Gunn diode was used as a mw source, and the power incident on the sample was varied in the range $0 < P_{\rm mw} \leqslant 50$ mW. The mw power reflected from the sample was modulated by the photoexcitation, and the modulation signal (measured by a lock-in amplifier) was proportional to the mw power absorbed by the sample (amounting to only $\leqslant 5\%$ of the incident power[22]). An external dc magnetic field was applied perpendicularly to the QW planes and its intensity was swept over the range $0 \leqslant B \leqslant 1$ T. The sample was photoexcited with either a He-Ne laser ($E_L = 1.96$ eV, $I_L < 10$ mW/cm^2) or a dye laser ($1.4 \leqslant E_L \leqslant 1.7$ eV, $I_L < 10$ mW/cm^2). Both the exciting laser beam and the PL emission traveled perpendicularly to the QW planes through a pinhole in the mw cavity. The PL signal was measured simultaneously with the PMA signal. The excitation was modulated by using an acousto-optic head at a frequency varying in the range of 10-10^5 Hz.

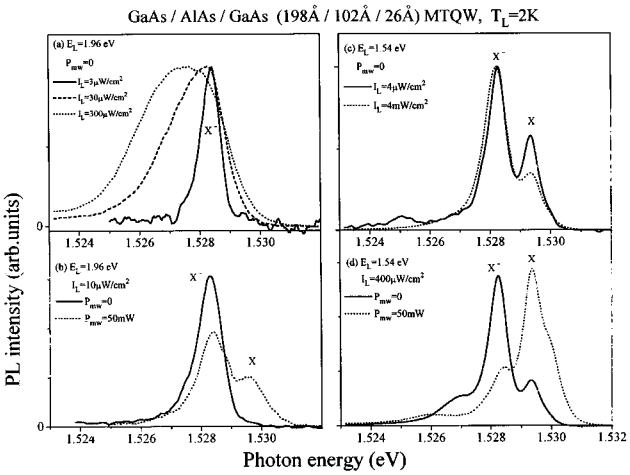

FIG. 1. PL spectra: (a) Excited at $E_L > E_g(e1\text{-hh1})_N$ and for three laser intensities. (b) Same E_L as in (a), with and without mw irradiation. (c) Excited at $E_g(e1\text{-hh1})_W < E_L < E_g(e1\text{-hh1})_N$ and for two laser intensities. (d) Same E_L as in (c), with and without mw irradiation.

The main investigation was done on the MTQW where the excitations studied were the X, X^-, and 2DEG that are created in the wide QW's as well as free holes generated in the narrow QW's. The excitations of the wide wells are introduced here by their PL and PL excitation (PLE) spectra. Figure 1(a) shows the PL spectra of the MTQW observed at 2 K under photoexcitation into the narrow wells [$E_L > E_g(e1\text{-hh1})_N \sim 1.9$ eV]. A single PL band is observed, with a broadening of its low-energy tail as I_L increases. Figure 1(b) shows that under microwave irradiation and for low I_L, a second PL band appears (at ~ 1.15 meV higher energy). These two PL bands were identified as X (the high-energy band) and X^- (the low-energy band).[13,21] Under photoexcitation below the narrow well band gap [Figs. 1(c) and 1(d)], the X and X^- bands are also observed, with relative intensities that depend on either I_L or $P_{\rm mw}$. Note that a weak low-energy band appears below the X^- band. It shifts toward low energy and disappears with mw power increase.

In order to further examine the effect of the 2DEG presence in the wide wells of the MTQW on the PL spectra and on the PMA dependence on B, we used the two-beam photoexcitation modulation technique. The MTQW sample is irradiated by two laser beams, both impinging on the same spot. A cw beam at $E_{L1} = 1.96$ eV generates a 2DEG in the

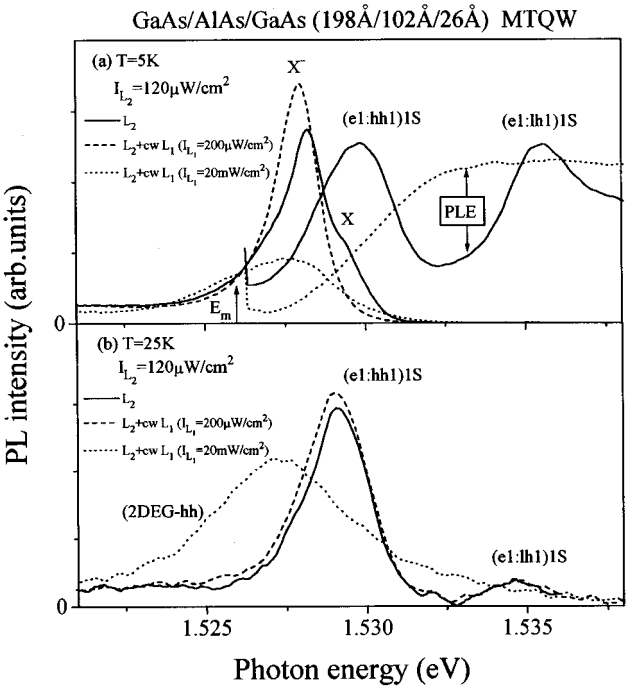

FIG. 2. (a) The photomodulated PL spectra excited simultaneously into the wide QW's (at $E_{L2}=1.54$ eV) with additional cw excitation into the narrow QW's (at $E_{L1}=1.96$ eV). The corresponding PLE spectra, monitored at E_m, are also shown. (b) Same as in (a), but at $T_L=25$ K.

wide QW's. Another, modulated beam, with $E_{L2}=1.54$ eV, mainly generates e-h pairs in the wide QW's. Then, only the modulated PL and PMA signals are detected by the lock-in amplifier, and the results are shown in Figs. 2 and 6.

Figures 2(a) and 2(b) show the photomodulated PL spectra for different intensities I_{L1} and at two temperatures. I_{L2} is set so that both the X and X^- PL bands are observed. (Under these conditions both the e- and X^--CR bands are observed in the PMA dependence on B, as discussed below.) Figure 2(a) shows that, as I_{L1} increases, the X-band disappears, whereas the X^- band broadens. The photomodulated PLE spectrum, monitored at E_m in the low-energy side of the X^- band, shows strong excitonic bands for low I_{L1} and a steplike spectrum, characteristic of a QW with 2DEG, for high I_{L1}. Figure 2(b) shows that, at $T_L \geqslant 20$ K, the transformation with increasing I_{L1} of the X band into the 2DEG PL occurs without the appearance of an intermediate X^- phase.

As will be discussed in Sec. III, the PMA is due to the photoexcited electrons (e) and X^- in the wide QW's and to heavy holes (hh) in the narrow QW's. Figures 3(a)–3(e) show the PMA dependence on magnetic-field strength (applied perpendicularly to the QW plane), measured under the same excitation conditions and at different temperatures. The corresponding PL spectra are shown in Figs. 3(f)–3(j). In order to analyze the line shape of the PMA dependence on B, we use the following expression for the power absorption of linearly polarized mw radiation having a frequency ω and an electric-field strength $E(\omega)$ (that is due to an electron rotating in the magnetic field B) in the classical case:[23]

$$P_{MA}(B)=\frac{ne^2\tau}{m^*}\,|E(\omega)|^2\,\frac{1+(\omega^2+\omega_c^2)\tau^2}{[1+(\omega^2-\omega_c^2)\tau^2]^2+4\omega_c^2\tau^2}. \tag{1}$$

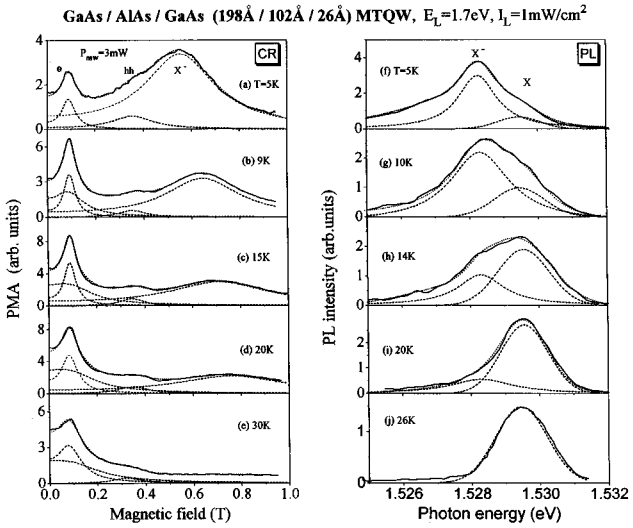

FIG. 3. Magnetic-field dependence of the photoinduced microwave absorption [(a)–(e)] and PL spectra [(f)–(j)] measured at five different temperatures. The deconvolution into electron, hole, and trion cyclotron resonances [in (a)–(e)] and into exciton and trion bands [in (f)–(j)] is shown by dashed lines. The dotted lines (virtually overlapping the experimental curves) are the fitted sums of all components.

Here $\omega_c=eB/m^*$ is the cyclotron frequency, n, m^*, and τ are the density, effective mass, and momentum relaxation time of the charged particle, respectively. Then each trace is fitted by adding several curves (depending on the number of observed resonances), which are calculated according to Eq. (1) and are shown by dashed lines in Figs. 3 and 4. Their sum is shown by a dotted line that virtually overlaps the experimental trace. Note that for $T_L>8$ K [Figs. 3(b)–3(e)]

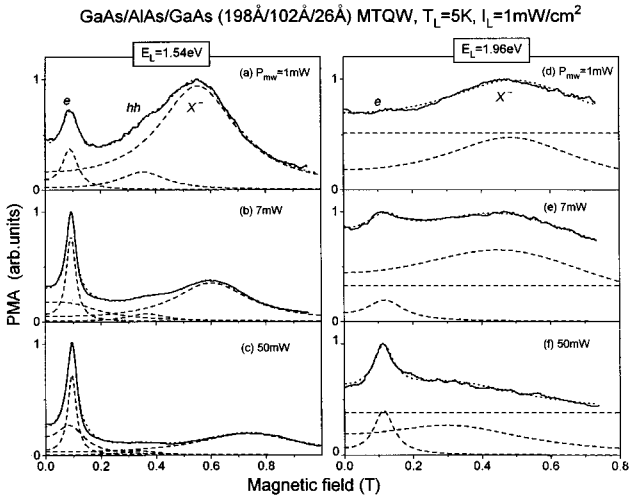

FIG. 4. Magnetic-field dependence of the photoinduced microwave absorption for three values of incident mw power. (a)–(c) Photoexcitation into the wide wells (at $E_L=1.54$ eV). (d)–(f) Photoexcitation into the narrow wells (at $E_L=1.96$ eV). The deconvolution into separate cyclotron resonances is shown by dashed lines. The dotted lines are the fitted sums of all components. In fitting curves (d), (e), and (f), an offset level (shown by the horizontal dashed lines) must be included. Note that for photoexcitation into the wide wells, all the lines are narrower than those observed under photoexcitation into the narrow wells.

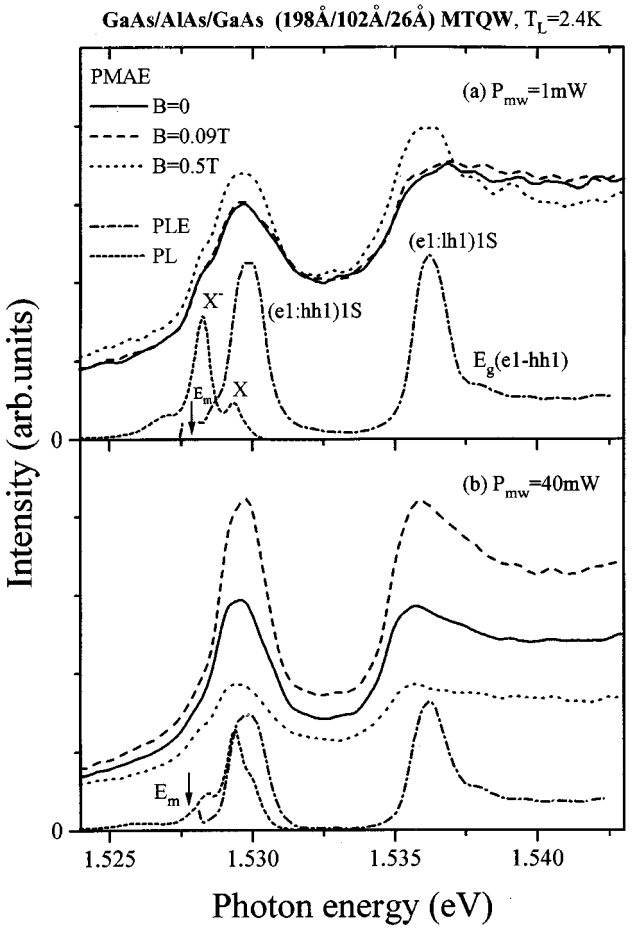

FIG. 5. The PLE spectrum monitored at E_m and the photoinduced microwave absorption excitation (PMAE) spectra obtained under low (a) and high (b) levels of incident mw power. The PL spectra excited at $E_L = 1.54$ eV are also shown. The PMAE spectra are observed at $B = 0$ and with an applied magnetic-field strength of the e-CR and X^--CR (0.09 and 0.5 T, respectively).

the fit requires an additional broad curve peaking at low B (<0.1 T) and having a low $\omega_c\tau$ (<1).

The PL spectra are similarly fitted by using a Voigt lineshape function, namely, a Lorentzian-Gaussian convolution $[I_{\mathrm{PL}}(E) = \int G(E')L(E-E')dE']$, for each PL band. The best fit to the PL spectra is obtained by taking the X^- line shape to be a Lorentzian and the X line shape to be a Gaussian.[21] The results of the PL spectra fitting are shown by the dashed curves for each band and by the dotted curves for their sum [Figs. 3(f)–3(j)].

The effect of increasing P_{mw} on the PMA dependence on B is shown in Figs. 4(a)–4(c) (for the case of photoexcitation into the wide QW's) and in Figs. 4(d)–4(f) (for photoexcitation above the narrow-well band gap). The fitting procedure is the same as that used in Fig. 3. As observed in the PL spectra [Figs. 1(b) and 1(d)], the X^--CR intensity decreases with increasing P_{mw}, while the e-CR intensity becomes dominant. Note that under photoexcitation with $E_L > E_g(e1\text{-hh1})_N$, the CR bands are broader than those observed for excitation at $E_L < E_g(e1\text{-hh1})_N$, and these bands ride on an additional, broad ''background'' signal. It is also observed that for the former E_L, as I_L increases, the e-CR intensity increases relative to that of the X^--CR, and both

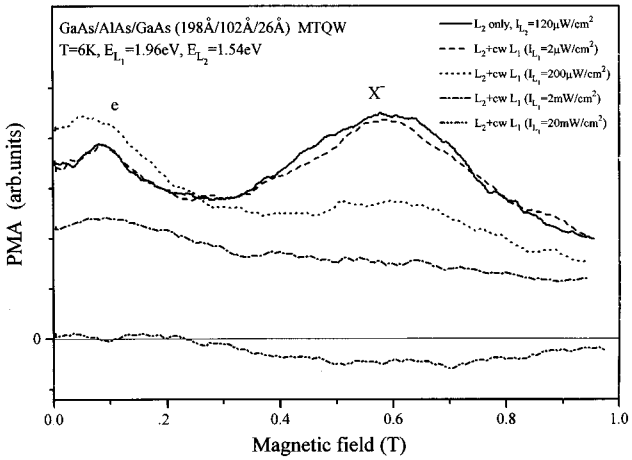

FIG. 6. Magnetic-field dependence of the photomodulated microwave absorption observed under photoexcitation into the wide QW's at $E_{L2} = 1.54$ eV (solid curve). The other four curves were obtained with an additional excitation into the narrow QW's at $E_{L1} = 1.96$ eV.

show increased broadening (not shown).

Since the PMA intensity depends on the charged particle (e, hh, and X^-) densities while that of the PL depends on the X and X^- densities, it is of interest to compare the excitation spectra of the PMA and PL [denoted PMAE and PLE, respectively, in Figs. 5(a) and 5(b)]. The PMAE spectra of Fig. 5(a) are measured at $B = 0$ and at the two magnetic-field strengths corresponding to the peak of the e- and X^--CR bands and for low P_{mw}. The excitation spectra of Fig. 5(b) are observed under intense mw irradiation. (The PL spectra taken under the same conditions are also shown.) While all excitation spectra show bands peaking at the $(e1\text{:hh1})1S$ and $(e1\text{:lh1})1S$ excitons, there are clearly differences between the PLE and PMAE spectra. These will be discussed in Sec. III.

The effect of increasing the 2DEG density in the wide QW's by exciting into the narrow QW's on the photomodulated CR traces is shown in Fig. 6. In this experiment, a two-beam excitation is used (as in Fig. 2). As the intensity of L_1 increases, the e-CR increases relative to the X^--CR, and both bands broaden. At high I_{L1} (lowest curve), the photomodulated part of the PMA signal cannot be separated from its cw part and no clearly resolved CR bands are observed.

Finally, we note that the PL spectra of the type-I MQW (used as a reference) did not show a line due to charged excitons. The PMA dependence on magnetic field showed a clear e-CR and a weak and broad background absorption. We thus conclude that, in our set of samples, the MTQW structure is essential for obtaining charged excitons under resonant excitation into the wide QW's.

III. ANALYSIS

In this section we analyze the experimental data along the following lines: (1) The PMA dependence on magnetic field is compared with the PL spectra in order to identify each component of the cyclotron resonance traces; (2) the e and X^- effective-mass variation with T_L and P_{mw} is analyzed in terms of weak in-plane localization; (3) the effect of

in-plane particle localization on the relative intensity of the CR and PL bands; (4) the e and X^- momentum relaxation-time dependence on T_L.

A. Identification of the photoexcited particles

The two PL bands, denoted X and X^-, that are shown in Fig. 1, were previously identified[13,20] as due to the radiative recombination of $(e1{:}\mathrm{hh}1)1S$ excitons and $[(e1{:}\mathrm{hh}1)1S+e]$ negatively charged excitons, respectively. As Fig. 1(a) shows, photoexcitation into the narrow QW's [at $E_L > E_g(e1\text{-}\mathrm{hh}1)_N$], gives rise only to the X^- band at $T_L = 2$ K. With increasing photoexcitation intensity ($I_L \geqslant 30\ \mu\mathrm{W/cm^2}$), X^- develops into a broad band that is characteristic of the 2DEG-hh recombination.[11,12] According to the experimentally determined[21] relation $n_e(I_L)$ we deduce that, in this case, the 2DEG density is $n_e > 5\times10^{10}\ \mathrm{cm^{-2}}$. However, as Figs. 1(c) and 1(d) show, in the case of the MTQW, even resonant excitation in the spectral range of the wide-well band gap [at $E_g(e1\text{-}\mathrm{hh}1)_W \sim 1.53$ eV] generates a low-density ($\leqslant 10^{10}\ \mathrm{cm^{-2}}$) 2DEG. These electrons are manifest in the X^- PL band and in the e-CR line [at $B \sim 0.09$ T, Figs. 3(a)–3(e) and 4(a)–4(c)]. This definite observation of a 2DEG indicates that a GaAs/AlAs MTQW excited near $E_g(e1\text{-}\mathrm{hh}1)_W$ differs from a conventional type-I MQW. We do not observe any charged exciton PL in our type-I MQW's. This means that electron-hole generation, without spatial separation of the electrons and the holes, results in efficient exciton formation. Only when some photoexcited electrons and holes are spatially separated, an exciton can bind an additional electron and form X^-. The MTQW structure provides such an efficient electron-hole separation since even below band gap photoexcitation can generate e-h pairs in the narrow wells. Comparing the relative intensities of the X and X^- PL bands [Figs. 1(a) and 1(c)] clearly shows that under photoexcitation into the wide QW's of the MTQW, the efficiency of X^- generation is much lower than that of direct excitation into the narrow QW's. A possible mechanism for creating excess electrons in the wide wells under excitation at $E_L < E_g(e1\text{-}\mathrm{hh}1)_N$ might be either carrier photoexcitation out of deep impurity centers or a two-step photoexcitation. Both processes must occur in the narrow QW's. It is noted that Osborne *et al.*[15] did observe X^+ PL in undoped type-I MQW and suggested that the excess holes arise from background carbon acceptors (that are present in their QW barriers).

The results of the two-beam experiments, presented in Fig. 2(a) further support this analysis. Increasing I_{L1} (excitation into the narrow wells) results in a 2DEG density increase. Then, the X band disappears, whereas the X^- band first broadens and then transforms into a broad PL band characteristic of a 2DEG-hh recombination.[11,12] At high temperatures [$T_L \geqslant 20$ K, Fig. 2(b)] and under relatively low I_{L1}, both $(e1{:}\mathrm{hh}1)1S$ and $(e1{:}\mathrm{lh}1)1S$ PL bands are observed (and no X^- band). The photomodulated PLE spectrum (at low I_{L1} and $T_L = 5$ K) shows very-well-resolved exciton bands. At high I_{L1}, the PLE spectrum is characteristic of a high-density 2DEG (an inhomogeneously broadened step function), as shown in Fig. 2(a). We thus establish that X and X^- as well as 2DEG are photoexcited in the wide wells and their relative PL intensity can be varied by varying I_{L1}.

We now turn to analyze the effects of the mw irradiation. In general, mw absorption by free carriers can be divided into nonresonant absorption (for example, at $B=0$) and resonant absorption (at the CR conditions). Equation (1) shows that the mw absorption at $B=0$ is nonzero for mobile carriers. This results in nonresonant carrier heating, and they impact activate excitons from localized into delocalized states.[24,25] In addition, carrier heating by mw absorption affects both their scattering and recombination rates.[26,27] Resonant mw absorption, apart from providing efficient carrier heating, is usually used for carrier identification, since the CR magnetic field is proportional to the carrier effective mass. The curve-fitting analysis of the CR traces shown in Figs. 3 and 4 indicates that there are at most four CR bands with relative intensities that depend on the experimental conditions. The CR band at $B \sim 0.09$ T is observed in both MTQW's and in our type-I MQW's and is due to electrons.[28] The CR band at $B \sim 0.5$ T is attributed to X^-, since its quenching with increasing temperature or with increasing mw power is similar to that of the X^- PL band.

A comparison between the various excitation spectra provides important information on free-carrier photogeneration. Figure 5 shows that both the PMAE and PLE spectra reveal strong $(e1{:}\mathrm{hh}1)1S$ and $(e1{:}\mathrm{lh}1)1S$ excitonic bands as well as an absorption onset at $E_g(e1\text{-}\mathrm{hh}1)_W$. While it is clear that the exciton bands are dominant in the PLE spectra, their appearance in the PMAE spectra indicates that the strong absorption is followed by a nonthermal exciton dissociation and spatial separation of the electron and hole. However, in contrast to the PLE case, the PMAE spectra show that free carriers are generated even for $E_L < E\ [(e1{:}\mathrm{hh}1)_W 1S]$ of the wide QW's. This means that free carriers are photoexcited out of deep traps.

We observe differences in the relative intensities of the PMAE spectra measured at $B=0$, $B \sim 0.09$ T, and $B \sim 0.5$ T. ($B \sim 0.09$ T and $B \sim 0.5$ T are the e-CR and X^--CR fields at $T_L = 5$ K, respectively, as seen in Figs. 3 and 4.) At low mw power, when only the X^--CR band is observable in the PMA dependence on B, the PMAE spectrum, observed under the e-CR field, coincides with that observed at $B=0$. On the other hand, the PMAE spectrum observed under the X^--CR field is stronger, as shown in Fig. 5(a). At high mw power [Fig. 5(b)], the e-CR is the most pronounced band in the PMA dependence on B, and this leads to a PMAE spectrum that is stronger than those observed at $B=0$ and 0.5 T. Thus, an increased e or X^- resonant heating increases the photoexcitation efficiency of these particles. This might be due to their increased mobility as they are activated from in-plane localizing regions (see below).

The PL spectra [shown in Fig. 1(d)] contain two additional weak bands, one of them at ~ 1.530 eV and the other is in the range of 1.525–1.527 eV. The latter shifts to low energy and disappears with mw power increase. We attribute this low-energy PL band to the recombination of localized electrons (the effects of carrier localization will be discussed later). The high-energy band appears only at high mw power, and, thus, it is assigned to free exciton recombination. The exciton delocalization under high power mw irradiation is confirmed by comparing the PL and the PLE spectra, shown in Fig. 5(b). The PLE spectrum monitored at the low-energy

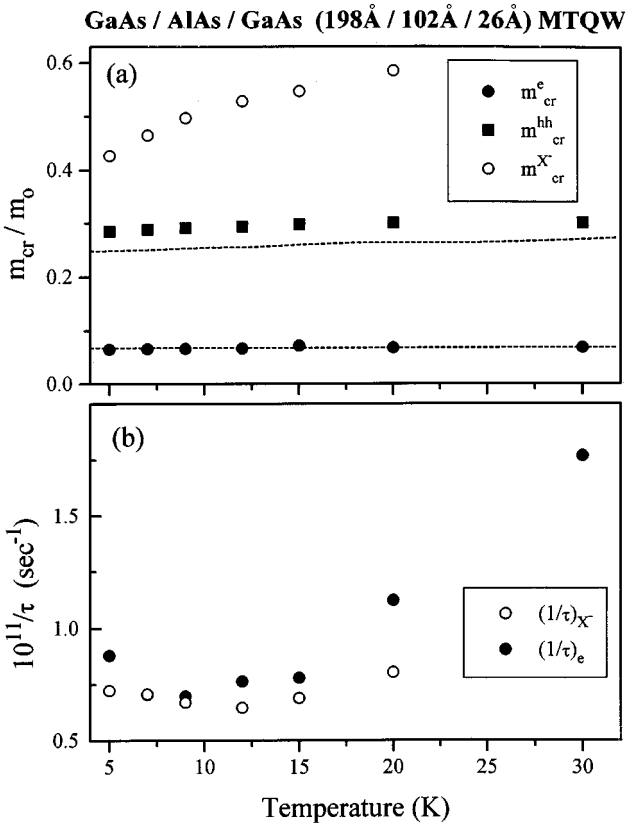

FIG. 7. Temperature dependence of the charged particles parameters (deduced from the photomodulated microwave absorption dependence on B) that are photoexcited in the MTQW and obtained by fitting the CR traces [as in Figs. 3(a)–3(e)]: (a) CR masses of e and X^- in the wide wells and hh in the narrow wells. The dashed lines are the calculated electron effective mass in the wide QW's (lower line) and heavy-hole effective mass in the narrow QW's (upper line). (b) The inverse momentum relaxation times of e and X^- as a function of temperature.

X^- tail (at E_m), shows strong excitonic bands and the onset of the ($e1$-hh1) continuum. The absence of a Stokes shift between the PL at 1.530 eV and the ($e1$:hh1)$1S$ exciton peak in the PLE spectrum is taken as evidence that it is the free exciton PL band.

B. Effective masses of the charged particles

The CR curve fitting yields the cyclotron mass of the e, hh, and X^-, and the momentum relaxation time of the e and X^-. (The hh signal is too weak for a reliable analysis of its broadening.) The extracted cyclotron masses as a function of temperature are shown in Fig. 7(a). We attribute the two lowermost CR's (at $B\sim0.09$ T and $B\sim0.37$ T) to electrons in the wide QW's and to heavy holes in the narrow QW's, respectively. The reasons are as follows: (a) Both of these CR bands persist up to high temperatures ($T_L>30$ K). (b) We calculated the effective masses (using the eight-band model of Baraff and Gershoni[29]). The calculated m_e (for a 200-Å-wide QW) and $m_{\rm hh}$ (for a 26-Å-wide QW) are shown by dashed lines and are very close to the values extracted from the experiment. (c) The calculated $m_{\rm hh}$ for a 200-Å QW does not agree with the observed CR value and, moreover, it is expected to be temperature dependent (in the range $2<T_L<30$ K) due to the hh1 and lh1 band anticrossing.

The heaviest cyclotron mass is that of the X^- in the wide QW's. It increases smoothly from $0.43m_0$ to $0.59m_0$ with T_L or $P_{\rm mw}$ increase up to those values that the X^--CR is unobservable. We know that the hh1-lh1 subband anticrossing results in in-plane effective masses that show a singularity like variation for low $k_\parallel$ ($<1.5\times10^6$ cm^{-1} for $d_W=200$ Å), namely, for very low in-plane energies [$\Delta E(k_\parallel)\leqslant3$ meV]. Therefore, the smooth variation of $m^{X^-}_{\rm cr}$ with T_L (or $P_{\rm mw}$) means that X^- should be considered as a complex having its own dispersion[30] that is more strongly affected by in-plane potential fluctuations (due to interface roughness) than by the constituent hh dispersion.

We observe that the in-plane $m^e_{\rm cr}$ varies in the range of $0.065m_0\leqslant m^e_{\rm cr}\leqslant0.070m_0$, when T_L increases from 2 to 30 K. (For a 200-Å GaAs QW, the calculated value of the in-plane electron effective mass is $m^*_e=0.068m_0$ at the bottom of the $e1$ subband.) It has been previously observed in various QW structures[16,31,32] that $m^e_{\rm cr}$ is not equal to the effective mass of the free in-plane particle. This was attributed to electron localization in the ''interface islands'' that arise from random potential fluctuations (remote donors or interface fluctuations[31,32]).

In order to provide an intuitive understanding of the in-plane localization effect on both the e-CR and X^--CR bands, we use the simple single-particle localization model,[33] wherein the random fluctuations are introduced by a finite set of harmonic-oscillator potentials with different characteristic frequencies ω_0. For charged particles, confined in such potentials and under an applied magnetic field, the electric dipole transitions occur at a shifted cyclotron frequency ω given by

$$\omega^2_{\rm cr}=\omega^2_c+(\omega^2_{of}-\omega^2_{oi}), \tag{2}$$

where $\omega_{\rm cr}=eB/m_{\rm cr}$, $\omega_c=eB/m^*$, $m_{\rm cr}$ and m^* are the cyclotron and effective carrier masses, respectively, $\hbar\omega_{of}$ and $\hbar\omega_{oi}$ are the final- and initial-state energies of the harmonic oscillator, respectively. In the case of free carriers, $m_{\rm cr}=m^*$. An intermediate state between full localization and free in-plane motion is that of a particle that is free to move over a large ''interface island'' (an area which is about $\pi r^2_{\rm cr}$). Thus, we explain the observed $m_{\rm cr}$ variation with T_L (or $P_{\rm mw}$) by a $\omega_{oi}\rightarrow\omega_{of}$ frequency shift when the carrier is promoted from ''islands'' with relatively strong localization to those with lesser localization ($\omega_{oi}>\omega_{of}$). This model requires that the length scale l of the potential fluctuations must be larger than the carrier cyclotron radius, in order to satisfy the criterion $\omega_c\tau>1$. For $l<r_{\rm cr}$, the carrier is too localized to be observed in mw CR ($\omega_c\tau<1$). For $l\gg r_{\rm cr}$, the potential fluctuation perturbation will be the same for both initial and final states of the CR transition, and the localization effect would not be observed.

C. Relative intensities of the CR and PL band

The CR curve fitting [Fig. 3(a)] shows that for $T_L>8$ K there appears a CR band that is due to low-mobility (lm) electrons ($\omega_c\tau\leqslant1$) *in addition* to that of high-mobility (hm) electrons ($\omega_c\tau\sim5$). For $T_L\leqslant5$ K, only the CR due to the

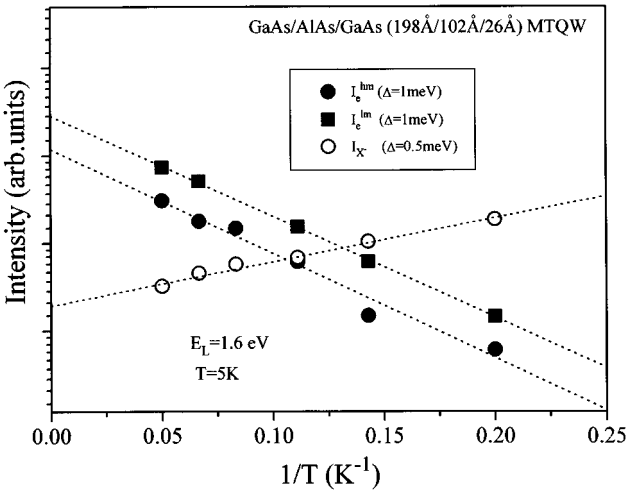

FIG. 8. Relative intensities of the high-mobility and low-mobility e-CR bands and X^--CR band as a function of the inverse temperature. The activation energies are deduced from the dependence: $\ln[I(T_L)]=-\Delta/k_BT_L+\text{const}$ (with a positive slope for X^--CR).

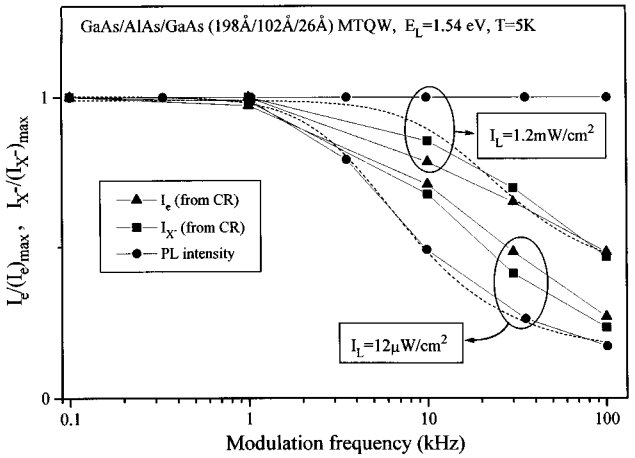

FIG. 9. Excitation modulation frequency dependence of the relative e-CR and X^--CR intensities and of the relative X and X^- PL band intensities. The dashed lines are the fitting curves obtained by using Eq. (3) with $\tau_1=4\times10^{-5}$ sec (low I_L) and $\tau_1=1.5\times10^{-5}$ sec (high I_L).

hm electrons is observed. This means that at low T_L a large fraction of the electrons are localized by in-plane potential fluctuations, so that they are not observable in the mw CR. [In the model described by Eq. (2) this means that the occupied oscillators have large ω_{oi} leading to $l<r_{cr}$, $\omega_c\tau<1$.] This is the reason for observing the e-CR and X^--CR bands with comparable intensities at low T_L (although the photoexcited e density is orders of magnitudes higher[13,21]). Then, with increasing T_L, lm electrons are thermally activated into localized states with much smaller ω_{of} and thus contribute to the CR signal. Similarly, for excitation at $E_L>E_g(e1\text{-}hh1)_N$, the ''background'' PMA signal [presented in Figs. 4(d)–4(f) by a virtually horizontal line] is attributed to a large density of lm electrons. Figure 8 shows the relative intensities of the hm and lm e-CR bands [integrated area under the CR trace that is extracted from the curve fitting of Fig. 3 using Eq. (1)] as a function of inverse temperature. Both the hm and the lm e-CR intensities increase with increasing temperature with an activation energy of ~1 meV. It is thus taken as an average localization energy. We note that a similar analysis of the e-CR intensity dependence on temperature for 50 Å-GaAs/$Ga_{0.7}Al_{0.3}As$ MQW's (Ref. 28) [where only a broad band ($\omega_c\tau\sim1.5$) is observed] yields an activation energy of ~2 meV. This is consistent with a previous study[16] that shows an electron localization energy increase with QW width decrease. Although the activation energy of ~1 meV for hm electrons correlates with the X^- binding energy ($E_{X^-}\sim1.15$ meV), it is more plausible to relate it to interface fluctuation in-plane islands since their density is much higher than that of X^-. A similar analysis of X^--CR intensity dependence on T_L, shown in Fig. 8, yields an activation energy (for X^- vanishment) of $\Delta=0.5$ meV. We note that the X^- binding energy, obtained from the spectroscopic data is more than twice the value of the X^- activation energy. Such a difference is frequently found in comparing spectroscopic and thermal binding energies and may be due to opening up of additional channels for X^- dissociation.

The in-plane localization effect can also be observed in the photomodulation frequency (ω_{mod}) dependence of the PL and CR band intensities, shown in Fig. 9. Both decrease with increasing ω_{mod} and under low photoexcitation intensity. It is interpreted as follows: Photogenerated unpaired electrons in the wide QW's are localized by random potential fluctuations that have a continuous distribution of ω_0. At low T_L, the electron lifetime in its localized states (τ_1) is long compared to the free-electron lifetime. Under low I_L, both the PL and CR intensity dependence on ω_{mod} can be fitted by[34]

$$I(\omega_{\text{mod}})\sim\frac{1}{[1+(\omega_{\text{mod}}\tau_1)^2]^{1/2}}, \tag{3}$$

with $\tau_1\sim4\times10^{-5}$ sec. As I_L increases, the localizing states are saturated. This results in a shorter τ_1 ($\sim10^{-5}$ sec for $I_L=1.2$ mW/cm^2) for the CR bands and in a PL intensity that is independent of ω_{mod}, since it results mainly from free X^- (as was reported in Ref. 21).

D. Electron and trion momentum relaxation times

Finally, the CR line-shape fitting [Eq. (1)] yields the carrier momentum relaxation times. Figure 7(b) shows the temperature dependence of $(1/\tau)_e$ and $(1/\tau)_{X^-}$ for the low-density 2DEG case. As the temperature increases to $T_L\sim12$ K, both relaxation times decrease slightly, then increase rapidly for $12<T_L<20$ K. Defining the corresponding in-plane mobilities at 35.6 GHz and $T_L=5$ K, we obtain $\mu_e\sim3\times10^5$ cm^2 V^{-1} sec^{-1} and $\mu_{X^-}\sim5\times10^4$ cm^2 V^{-1} sec^{-1}, respectively. For comparison, in ultrapure bulk GaAs, a very high electron mobility of $\sim1.5\times10^6$ cm^2 V^{-1} sec^{-1} (at $T_L=5$ K) was deduced from the mw CR line shape by using the same experimental technique.[35] In the bulk GaAs case the electron mobility is determined by acoustic-phonon (piezoelectric interaction) and neutral-impurity scatterings. Since the MTQW is nominally undoped, the fivefold decrease of its mobility relative to that of ultrapure bulk GaAs can be attributed mainly to interface roughness scattering and to the carrier-carrier scattering. The latter is explained by e-X^-

scattering[21] and by scattering of hm and lm electrons in the wide QW's. In addition, it is plausible to assume that e or X^- scattering is taking place by the holes (mobile or localized) in the narrow QW's. Note that the carrier-carrier scattering rate greatly increases with 2DEG density increase. Indeed, as Fig. 4 shows, the observed CR bands under photoexcitation into the narrow QW's are much broader (by a factor of ~ 3) than those observed under photoexcitation into the wide QW's. The two-beam excitation experiments (Fig. 6) also show an increased broadening of both electron and trion CR bands with increased photoexcitation intensity into the narrow QW's.

IV. CONCLUSIONS

We reported on a comparative study of the low-temperature PMA and PL spectra in a GaAs/AlAs MTQW system, in which spatially separated 2DEG and 2DHG are optically photoexcited, and their density is controlled by the photoexcitation intensity. At moderate photoexcitation intensities, we found the existence (in the wide QW's) of the mixed phase consisting of a low-density photoexcited 2DEG ($n_e < 5\times 10^{10}$ cm^{-2}) and much lower densities of X and X^-. While the interband (PL) transitions probe the X and X^- components of the mixed phase, the PMA dependence on the magnetic field (applied perpendicularly to the QW plane) probes the e and X^- components in the wide QW's and the hh in the narrow QW's through their CR's. The effect of increasing the lattice temperature or the electron temperature (by microwave heating) on the cyclotron mass shift and on the relative e-CR and X^--CR intensities is explained by particle localization in the ''interface islands'' of the random potential fluctuations. In our study, we used only one microwave frequency and tuned the CR with the magnetic field. In order to better understand the type of localizing potential (harmonic-oscillator potential or Coulomb binding potential), we plan to carry out similar CR experiments over a wide range of microwave frequencies.

ACKNOWLEDGMENT

The work at Technion was done in the Barbara and Norman Seiden Center for Advanced Optoelectronics. It was supported by the Israel Science Foundation (founded by the Israel Academy of Science and Humanities).

[1] D. Heiman, Semicond. Semimet. **36**, 2 (1992).
[2] A. J. Shields, M. Pepper, D. A. Ritchie, and M. Y. Simmons, Adv. Phys. **44**, 47 (1995).
[3] H. Yoshimura and H. Sakaki, Phys. Rev. B **39**, 13 024 (1989).
[4] G. D. Sanders and Y. C. Chang, Phys. Rev. B **35**, 1300 (1987).
[5] D. Huang, J. I. Chui, and H. Morkoc, Phys. Rev. B **42**, 5147 (1990).
[6] A. J. Shields, M. Pepper, D. A. Ritchie, M. Y. Simmons, and G. A. C. Johns, Phys. Rev. B **51**, 18 049 (1995).
[7] R. Harel, E. Cohen, E. Linder, Arza Ron, and L. N. Pfeiffer, Phys. Rev. B **53**, 7868 (1996).
[8] P. Hawrylak, Phys. Rev. B **44**, 3821 (1991).
[9] G. E. W. Bauer, Phys. Rev. B **45**, 9153 (1992).
[10] K. Kheng, R. T. Cox, Y. Merle d'Aubigne, F. Bassani, K. Saminadayar, and S. Tatarenco, Phys. Rev. Lett. **71**, 1752 (1993).
[11] G. Finkelstein, H. Shtrikman, and I. Bar-Joseph, Phys. Rev. Lett. **74**, 976 (1995).
[12] A. J. Shields, M. Pepper, M. Y. Simmons, and D. A. Ritchie, Phys. Rev. B **52**, 7841 (1995).
[13] Arza Ron, H. W. Yoon, M. D. Sturge, A. Manassen, E. Cohen, and L. N. Pfeiffer, Solid State Commun. **97**, 741 (1995).
[14] G. Finkelstein, H. Shtrikman, and I. Bar-Joseph, Phys. Rev. B **53**, R1709 (1996).
[15] J. L. Osborne, A. J. Shields, M. Pepper, F. M. Bolton, and D. A. Ritchie, Phys. Rev. B **53**, 13 002 (1996).
[16] R. J. Warburton, J. G. Michels, R. J. Nicholas, J. J. Harris, and C. T. Foxon, Phys. Rev. B **46**, 13 394 (1992).
[17] D. M. Hofmann, M. Drechsler, C. Wetzel, B. K. Meyer, F. Hirler, R. Strenz, G. Abstreiter, G. Bohm, and G. Weimann, Phys. Rev. B **52**, 11 313 (1995).
[18] M. Kozhevnikov, E. Cohen, Arza Ron, and L. N. Pfeiffer, *Proceedings of the 23rd International Conference on the Physics of Semiconductors, Berlin*, edited by M. Scheffler and R. Zimmermann (World Scientific, Singapore, 1996), p. 2183.
[19] I. Galbraith, P. Dawson, and C. T. Foxon, Phys. Rev. B **45**, 13 499 (1992).
[20] J. Feldmann, M. Preis, E. O. Goebel, P. Dawson, C. T. Foxon, and I. Galbraith, Solid State Commun. **83**, 245 (1992).
[21] A. Manassen, E. Cohen, Arza Ron, E. Linder, and L. N. Pfeiffer, Phys. Rev. B **54**, 10 609 (1996).
[22] B. M. Ashkinadze, E. Cohen, Arza Ron, and L. N. Pfeiffer, Phys. Rev. B **47**, 10 613 (1993).
[23] K. Seeger, in *Semiconductor Physics* (Springer-Verlag, Wien, 1973), Chap. 11.
[24] M. Godlewski, W. M. Chen, and B. Monemar, Crit. Rev. Solid State Mater. Sci. **19**, 241 (1994).
[25] M. Kozhevnikov, B. M. Ashkinadze, E. Cohen, and Arza Ron, Phys. Rev. B **52**, 4855 (1995).
[26] B. M. Ashkinadze, V. V. Bel'kov, and A. G. Krasinskaya, Fiz. Tekh. Poluprovodn. **24**, 883 (1990) [Sov. Phys. Semicond. **24**, 555 (1990)].
[27] E. Hanamura and T. Inui, J. Phys. Soc. Jpn. **17**, 666 (1962).
[28] A detailed account of the e-CR in QW's of various widths will be published elsewhere.
[29] G. A. Baraff and D. Gershoni, Phys. Rev. B **43**, 4011 (1991).
[30] K. Kheng, R. T. Cox, T. Baron, K. Saminadayar, and S. Tatarenco, J. Cryst. Growth **159**, 443 (1996).
[31] J.-P. Cheng and B. D. McCombe, Phys. Rev. B **44**, 3070 (1991).
[32] J. P. Kotthaus, G. Abstreiter, J. F. Koch, and R. Ranvaud, Phys. Rev. Lett. **34**, 151 (1975).
[33] H. J. Mikeska and H. Schmidt, Z. Phys. B **20**, 43 (1975).
[34] B. M. Ashkinadze, E. Tsidilkovski, E. Cohen, Arza Ron, and L. N. Pfeiffer, Phys. Rev. B **54**, 8728 (1996).
[35] M. Kozhevnikov, B. M. Ashkinadze, E. Cohen, and Arza Ron, Phys. Rev. B **52**, 17 165 (1995).